Open Ceramics 9 (2022) 100217

Contents lists available at ScienceDirect

Open Ceramics

journal homepage: www.sciencedirect.com/journal/open-ceramics

The early porcelain kilns of Arita: Identification of raw materials and their use from the 17th to the 19th century

Riccardo Montanari [a,*], Nobuyuki Murakami [b], Alberto De Bonis [c,d], Philippe Colomban [e], Maria Francesca Alberghina [f], Celestino Grifa [d,g], Francesco Izzo [c], Vincenzo Morra [c,d], Claudia Pelosi [h], Salvatore Schiavone [f]

[a] Independent Researcher, Expert Witness, Rome, Italy
[b] Arita Museum of History, Arita, Saga Prefecture, Japan
[c] Dipartimento di Scienze della Terra, dell'Ambiente e delle Risorse (DiSTAR), Università degli Studi di Napoli Federico II, Complesso Universitario di Monte Sant'Angelo, Via Cupa Nuova Cintia, 21, Napoli, 80126, Italy
[d] CRACS, Center for Research on Archaeometry and Conservation Science, Complesso Universitario di Monte Sant'Angelo, Via Cupa Nuova Cintia, 21, Napoli, 80126, Italy
[e] MONARIS, Sorbonne Université, CNRS, 4 Place Jussieu, 75005, Paris, France
[f] S.T.Art-Test sas, Italy
[g] Dipartimento di Scienze e Tecnologie, Università degli Studi del Sannio di Benevento, via De Sanctis snc, Benevento, 82100, Italy
[h] University of Tuscia, Laboratory of Diagnostics and Materials Science, Largo dell'Università, Viterbo, Italy

ARTICLE INFO

Keywords:
Japanese porcelain
Arita clay
Izumiyama
Ryumon
Shirakawa

ABSTRACT

Porcelain stone used at the early kilns of Arita, Japan, has never been identified due to the lack of written records. Ryumon and Shirakawa deposits are considered to have possibly been exploited before Izumiyama was discovered in the early 1630s, but there are no records or any previous scientific research aimed at resolving such crucial issue. This work presents the first systematic scientific study of clays from the three deposits and shards excavated at early kiln sites. Portable ED-XRF and SEM-EDS were used to identify the chemical compositions of bodies, glazes, and geochemical characteristics of clays. XRD, TG-DSC, and FTIR-ATR spectroscopy were also used for the mineralogical characterization of clay bodies. Results show that the earliest production was marked by the mineralogical characteristics of the available raw materials. A gradual improvement in material selection and processing will lead to the development of the *nigoshide* (milky-white) body in the mid-17th century.

1. Introduction

The production of Japanese porcelain owes its origin to the discovery of porcelain stone deposits by Korean potters who had been taken to Japan by Toyotomi Hideyoshi after the two Korean military campaigns (1592–98) [1,2]. Porcelain stone found in Arita deposits consists of highly silicic volcanic rocks, specifically rhyolites, that underwent hydrothermal alteration with a resulting varying presence of smectite, illite, kaolinite, feldspars and quartz, thus combining the properties suitable for the production of hard-textured ceramic wares (refer to section 2 for a detailed discussion).

There has been much debate regarding what type of raw material had actually been used in the earliest stage of porcelain production, but the lack of written records made it impossible to determine the characteristics of the materials employed for bodies and glazes in the kilns operating between 1610 and 1630 [3,4]. The sources of the materials would all have been located around the city of Arita, the porcelain production center of Japan in northwest Kyushu. The discovery of the Izumiyama quarry (located in the eastern part of Arita), the deposit used throughout the Edo period (1603–1868), occurred around the early 1630s [3,4]. No written records exist in relation to the other deposits close to Arita, namely, Ryumon and Shirakawa. Ryumon, located in the western part of Arita, is believed to have been used for a short period of time due to its highly poisonous arsenic content [1], yet no evidence is available as to if and when it had actually been exploited; while Shirakawa is believed to have been used for glaze production only.

In order to provide an answer to such crucial issues, we have carried out the first systematic scientific study of rocks from the three deposits,

* Corresponding author.
E-mail address: ckrm97@yahoo.com (R. Montanari).

https://doi.org/10.1016/j.oceram.2021.100217
Received 11 August 2021; Received in revised form 28 December 2021; Accepted 29 December 2021
Available online 2 January 2022

along with shards excavated at different kiln sites active from the 17th to the 19th centuries (mostly by non-destructive technique as a mandatory requirement): Komizo, Benzaiten, Tenjimori, Tengudani, Tenjinyama, Yanbeta, Kusunokidani, Hokaoyama, Nakashirakawa, Hirose, Aka-e machi, Kakiemon, Izumyama kuchiya basho, Nabeshima, Mukurodani, Tataranomoto, Hirosemukai.

The analytical techniques employed are portable Energy-Dispersive X-Ray Fluorescence (ED-XRF), Scanning electron microscopy/energy-dispersive X-ray spectroscopy (SEM/EDS), X-Ray Diffraction (XRD), Thermogravimetry with differential scanning calorimetry (TG-DSC), and FTIR-ATR spectroscopy. The aim was to identify the deposits from which Japanese potters sourced the raw materials needed for both bodies and glazes, with a particular focus on the earliest periods of production. The results offer, for the first time, definitive evidence regarding the origin of the materials available to the different kilns, and the study clearly shows how material selection and processing improved as potters gained experience after an initial period of experimentation. Furthermore, scientific evidence enabled us to identify the movement of potters between different kilns and track downthe development of the iconic high-grade *nigoshide* body (milky-white). The *nigoshide* body played a crucial role in the spread of Kakiemon wares in Europe at the end of the 17th century as its pure white and translucent nature emphasized the refined overglaze enamels that had previously been developed with the help and supervision of Jesuit missionaries by means of materials and technology imported into Japan from the Old Continent [5–7] before the enforcement of the isolation policy (*sakoku*) by the Tokugawa shogunate in 1639.

2. Clays of the Arita region

Clay deposits located in the vicinity of Arita, Northwest Kyushu, are formed by hydrothermal alteration of rhyolites (highly silicic volcanic rocks) intruded in Paleogene sandstone and shale [8,9] (Fig. 1a). Characteristics of this environment are both a zonation from the heat source, and a high variability of mineral contents over short distances. The minerals formed under such conditions are influenced by the chemical composition, pH and temperature of the fluid; and by the petrography of the host rocks [10].

2.1. Izumiyama deposit

Izumiyama deposit shows an approximately radial distribution of four different zones from the center to the outer alteration area (Fig. 1b) [8,10]. Mineralogical studies [11,12] have identified the constituent minerals of the four zones, which have then been divided accordingly: a vein of illite ($(K,H_3O,NH_4\ \ldots)(Al,Mg,Fe)_2(Si,Al)_4O_{10}$, zone 1), surrounded by increasing content of kaolinite ($Al_2Si_2O_5(OH)_4$, zone 2) and then poor transformed minerals (sanidine feldspar, plagioclase, zone 3 and 4); quartz being present everywhere. Smectite and Buddingtonite ($NH_4AlSi_3O_8$) are also observed in the outer zones.

The constituents in the Izumiyama deposit are illite issued from dioctahedral mica (hydromuscovite) and interstratified illite-smectite with typical interlayer cation K^+ and limited interlayer cation NH_4^+ [8,13]. Izumiyama illite is rich in Al, consistently with its dioctahedral nature [13] and poor in iron. Illite and smectite provide good plasticity to the clay [13]. Illite particles are very fine, and by acting as a flux throughout the porcelain body, and readily reacting with quartz and kaolinite at high temperature, they easily form a glassy phase containing mullite crystals ($T > 1200\ ^\circ C$), thus increasing the density of vitrification and translucency of the porcelain body [14,15]. The distribution of the different minerals determines the thermal properties of the stones [12].

3. Materials and methods

3.1. Analyzed shards and clays

All analyzed shards were provided by the Arita Museum of History, Arita, Saga Prefecture, Japan, and were excavated at kiln sites in Arita. Characteristics are summarized in Tables 1(a) and 1(b).

3.2. XRF spectrometer: experimental and measurement parameters

The employed XRF portable instrument consists of a miniature X-ray tube system, which includes the X-ray tube (max voltage of 40 kV, max current of 0.2 mA, target Rh, collimator 1 or 2 mm), the power supply, the control electronics and the USB communication for remote control; a Silicon Drift Detector (SDD) with a 125–140 eV FWHM @ 5.9 keVMn Kα line Energy Resolution (depends on peaking time and temperature); 1 keV–40 keV Detection range of energy; max rate of counts to 5.6×10^5 cps; Amptek DpppMCA software for acquiring the XRF spectra and OriginPro 8.5 for data processing.

Primary beam and detector axis form an angle of 0 and 40° respectively with the perpendicular to the sample surface. Measurement parameters were as follows: tube voltage 35 kV; current 80 μA, acquisition

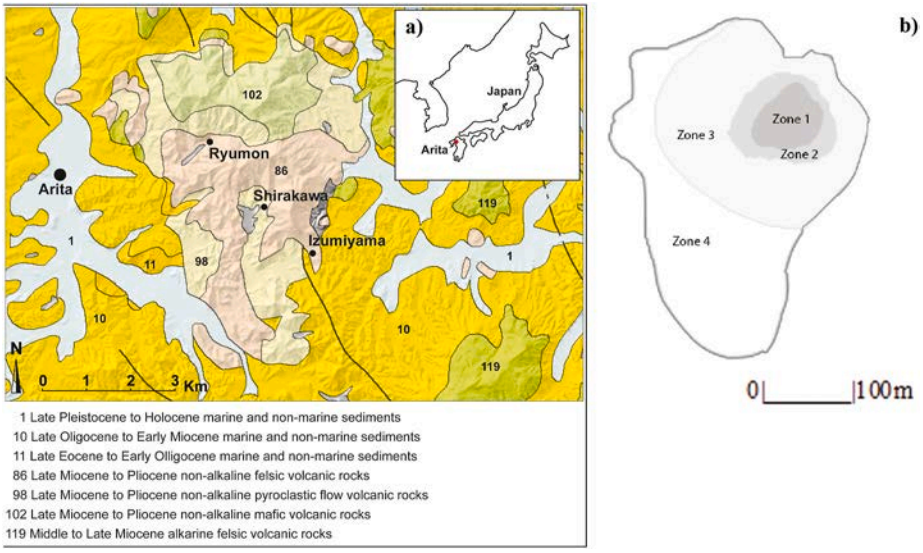

Fig. 1. (a) Geological sketch map of the Arita region (https://gbank.gsj.jp/seamless/seamless2015/2d/index.html?lang=en); (b) Radial distribution of the four alteration zones of Izumiyama deposit: Zone 1: Illite zone; Zone 2: Illite-Kaolinite zone; Zone 3: Weakly Altered Zone I; Zone 4: Weakly Altered Zone II.

Table 1
(a). Main characteristics of analyzed shards. (b). Analyzed rocks.

Kiln site	Number of samples	Period of production	Technology
Komizo	5	1610–1620	Underglaze blue decoration
	5	1620–1630	Underglaze blue decoration
Benzaiten	3	1610–1630	Underglaze blue decoration
Tenjinmori	5	1610–1630	Underglaze blue decoration
Tengudani	4	1630–1640	Underglaze blue decoration
	3	1640	Underglaze blue decoration
	3	1650	Underglaze blue decoration
Tenjinyama	1	1630–1640	Underglaze blue decoration
Yanbeta	3	1640–1650	Overglaze enamels decoration
	1		Underglaze blue decoration
Kusunokindani	2	1650	Nigoshide white body
Hokaoyama	2	1650	Underglaze blue decoration
Nakashirakawa	3	1660–1670	Underglaze blue decoration
Hirose	2	1650–1660	Underglaze blue decoration
Kakiemon	2	1670–1690	Nigoshide white body
	1	1670–1680	Underglaze blue decoration
Izumyamakuchiyabasho	2	1680–1690	Underglaze blue decoration
Izumiyama Kuchiya Bansho (VOC lettering)	1	1690–1710	Underglaze blue decoration
Nabeshima	1	1690–1730	Overglaze decoration
Mukurodani	2	1690–1700	Underglaze blue decoration
	3	1730–1740	Underglaze blue decoration
Tataranomoto	3	18th century	Underglaze blue decoration
Hirosemukai	2	19th century	Underglaze blue decoration

Clay deposit site	Number of analyzed deposit samples
Ryumon	9
Shirakawa	4
Izumiyama	3

time 100s; no filter was applied between the X-Ray tube and the sample; distance between sample and detector around 1 cm. The setup parameters were selected to have a good spectral signal and to optimize the signal to noise ratio (SNR).

3.3. XRD spectrometer: experimental and measurement parameters

Measurements were carried out with a BRUKER D2 PHASER 2nd generation diffractometer with the following operating conditions: CuKα, 30kVV, 10 mA; 4–50° 2θ, scanning interval (3–50° 2θ for the oriented aggregate), time per step 1 s, step size 0,02° 2 theta.

Mineralogical analyses were carried out on six representative samples (IZU1, IZU2, SHI1, RYU-A, RYU-B, RYU-C) of raw materials from the investigated deposits. The analysis was performed via X-ray diffraction (XRD) on powdered samples for the qualitative determination of the bulk mineralogy and on the clay fraction (<2 μm) separated via sedimentation in pure water following the Stokes law [16]. The analysis of the clay fraction was performed on the oriented aggregates after air-drying and after thermo-chemical treatment (ethylene glycol solvation, 550 °C heating) in order to better characterize the clay minerals [17].

3.4. SEM-EDS

Analysis was performed by means of a SEM Zeiss EVO HD15 (Carl Zeiss, Oberkochen, Germany), operating at 20 kV accelerating voltage, 200 pA I probe current and spot size of 429 μm, equipped with an Oxford Instruments Microanalysis Unit (Xmax 80 EDS detector). Smithsonian Microbeam Standards were used for EDS calibration. Selected shards of porcelain bodies were analyzed via scanning electron microscopy/energy-dispersive X-ray spectroscopy (SEM/EDS) microanalyses on carbon-coated and polished thin sections. The microchemical analysis was performed on areas (five measurements per sample) of polished fragments of porcelain to obtain the quantitative chemical composition of the ceramic matrix.

3.5. Thermal analyses

Clays (both bulk and <2 μm samples) have been thermally analyzed (Thermogravimetry TG and Differential Scanning Calorimetry DSC) by means of a NETZSCH Jupiter STA499 F3 Jupiter instrument using alumina crucibles. Samples were heated from room temperature to 1050 °C, at a heating rate of 10 °C/min in ultra-pure air (80% N_2; 20% O_2) atmosphere (flow 60 mL/min).

3.6. Infrared spectroscopy

FTIR-EGA were carried out by means of a BRUKER Tensor 27 instrument, coupled to the STA 449 F3 apparatus by a transfer line heated at temperature of 200 °C. Netzsch Proteus 6.1.0 (NETZSCH-Gerätebau GmbH) and Opus 7.2 software (Bruker Optics GmbH) were used for data analysis.

Starting materials and SMZNs were also examined with a Bruker Alpha FTIR spectrometer in Attenuated Total Reflectance (ATR) mode (128 scans at spectral resolution of 4 cm^{-1} in a spectral range of 400–4000 cm^{-1}). Processing of spectra was carried out by Opus 7.2 software (Bruker Optics GmbH).

4. Results and discussion

4.1. The raw materials

4.1.1. Izumiyama, Ryumon and Shirakawa: mineralogical features of raw materials via XRD, thermal analyses, and FTIR

XRD for the analyzed raw materials are reported in Fig. 2. Table 2 lists their constituent minerals.

Samples from the Izumiyama quarry (IZU1 and IZU2) are characterized by abundant quartz (Fig. 2a and b), with a scarce amount of feldspar detected in the IZU1 sample (Fig. 2a). Clay minerals identified with the method of oriented aggregates show illite/muscovite phase observed in correspondence of the reflections at about 10 and 5 Å d-spacing in both IZU1 and IZU2 specimens (Fig. 2a and b). Smaller amounts of kaolinite were also detected in IZU1 with characteristic Bragg peaks at approximately 7.12 and 3.57 Å d-spacing, which disappeared after heating to 550 °C due to the dehydration and collapse of the crystal structure of this phase (Fig. 2a). Results prove perfectly consistent with previous studies [8,9] and the radial distribution of the alterations zones reported in Fig. 1b.

The specimens collected from the Ryumon deposit show some differences from one another. Sample RYU-A contains polymorphs of silica represented by quartz and cristobalite; feldspar was also detected in subordinate amounts (Fig. 3a).

The sample from the Shirakawa deposit (SHI2) is characterized by

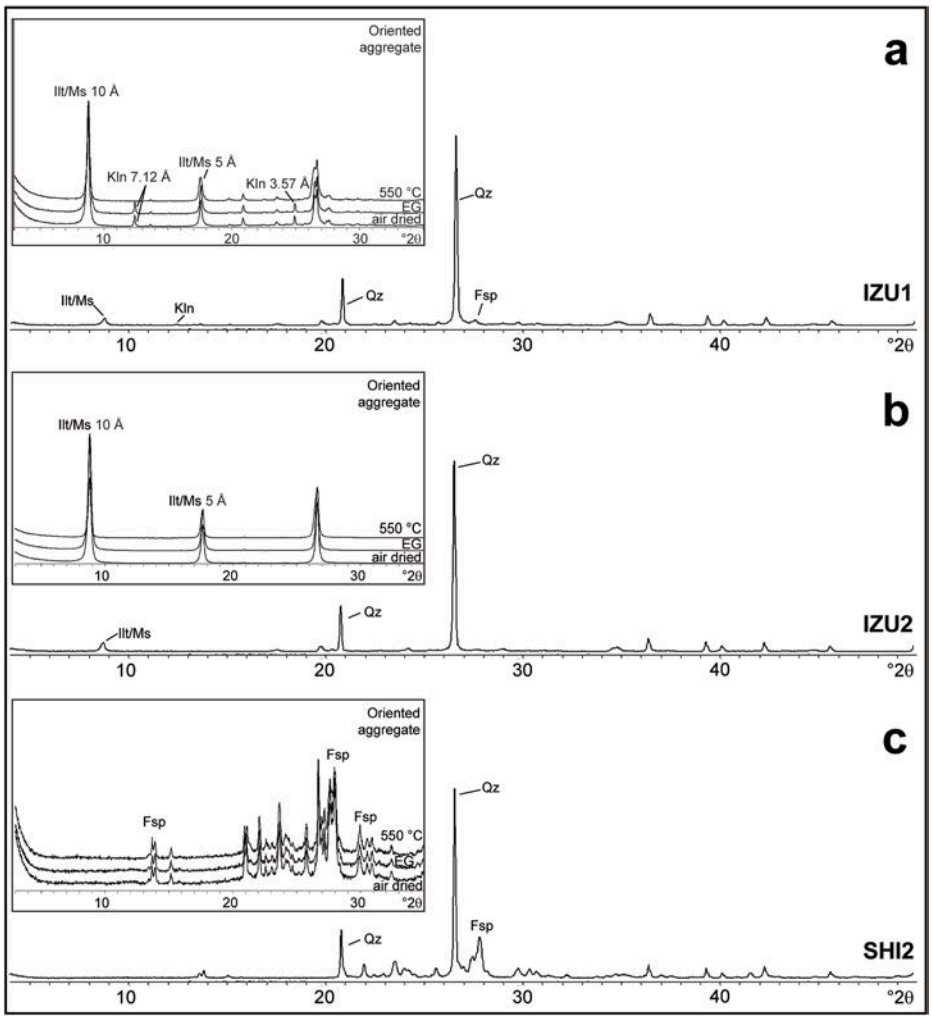

Fig. 2. XRD patterns for the analyzed raw materials. Bulk and oriented aggregates, air-dried, ethylene glycol solvated (EG), and heated to 550 °C of clay fraction (inset at the top left corner). (a) IZU1, (b) IZU2, (c) SHI2. Abbreviations of minerals according to Whitney and Evans (2010): Qz, quartz; Fsp, feldspar; Ms, muscovite; Ilt, illite; Kln, kaolinite.

Table 2
Constituent minerals of the raw materials analyzed by XRD.

Sample	Non-plastic Minerals	Clay Minerals
IZU1	Quartz, Feldspar	Illite, Kaolinite (Very limited illite interlayer cation NH_4^+ detected by FT-IR analysis)
IZU2	Quartz	Illite (Very limited illite interlayer cation NH_4^+ detected by FT-IR analysis)
RYU-A	Quartz, Cristobalite, Feldspar (Sanidine/ Orthoclase, Plagioclase)	Interstratified Illite-Smectite with high smectite content (10% illite - 90% smectite)
RYU-B	Quartz, Feldspar (Sanidine/ Orthoclase, Plagioclase)	Interstratified Illite-Smectite IS80R1 with high illite content (80% illite - 20% smectite), Corrensite
RYU-C	Quartz, Feldspar (Sanidine/ Orthoclase, Plagioclase)	Interstratified Illite-Smectite (60% illite - 40% smectite) IS60R1 (Very limited illite interlayer cation NH_4^+ detected by FT-IR analysis)
SHI2	Quartz, Feldspar (Plagioclase)	–

quartz and minor feldspar, with no appreciable amounts of clay phases (Fig. 2c).

The analysis of the clay fraction of RYU-A revealed the presence of an illite-smectite mixed-layered phase with a high amount (>90%) of the expandable smectitic component. The presence of smectite is evidenced by the low angle part of the pattern measured by reflection-diffraction set-up with characteristic intense bands at approximately 15 Å of the air-dried sample and about 17 Åd-spacing after ethylene glycol (EG) solvation (Fig. 3a). However, the smectite interlayer can host a large amount of species that give large expansion along the axis perpendicular to the phyllosilicate slab.

Sample RYU-B is composed of quartz and subordinate feldspar. Clay minerals are again represented by mixed-layers. In particular, the measurement of the differential parameter Δ2θ [17] between the diffraction effects after EG-solvation at approximately 17.05 2θ (5.2 Å) and 9.172θ (9.6 Å) (Fig. 3b) indicated the presence of an illite-smectite IS80R1, characterized by 80% illite and statistical stacking order (*Reichweite*) R1. Reflections at about 15.2 Å and 7.6 Å visible after EG solvation and at 11.4 Å after heating to 550 °C indicate the presence of another interstratified phase chlorite-smectite identifiable as corrensite (Fig. 3b).

Sample RYU-C is again formed of quartz and minor feldspar along with mixed-layered clay minerals. In this case the analysis showed the presence of superstructures at about 13.3 Å and 27 Å and the differential parameter Δ2θ [17] between reflections at about 16.60 2θ (5.3 Å) and 9.59 2θ (9.2 Å) in the EG-solvated sample (Fig. 3c) indicated an illite-smectite mixed-layer IS60R1, characterized by 60% illite and

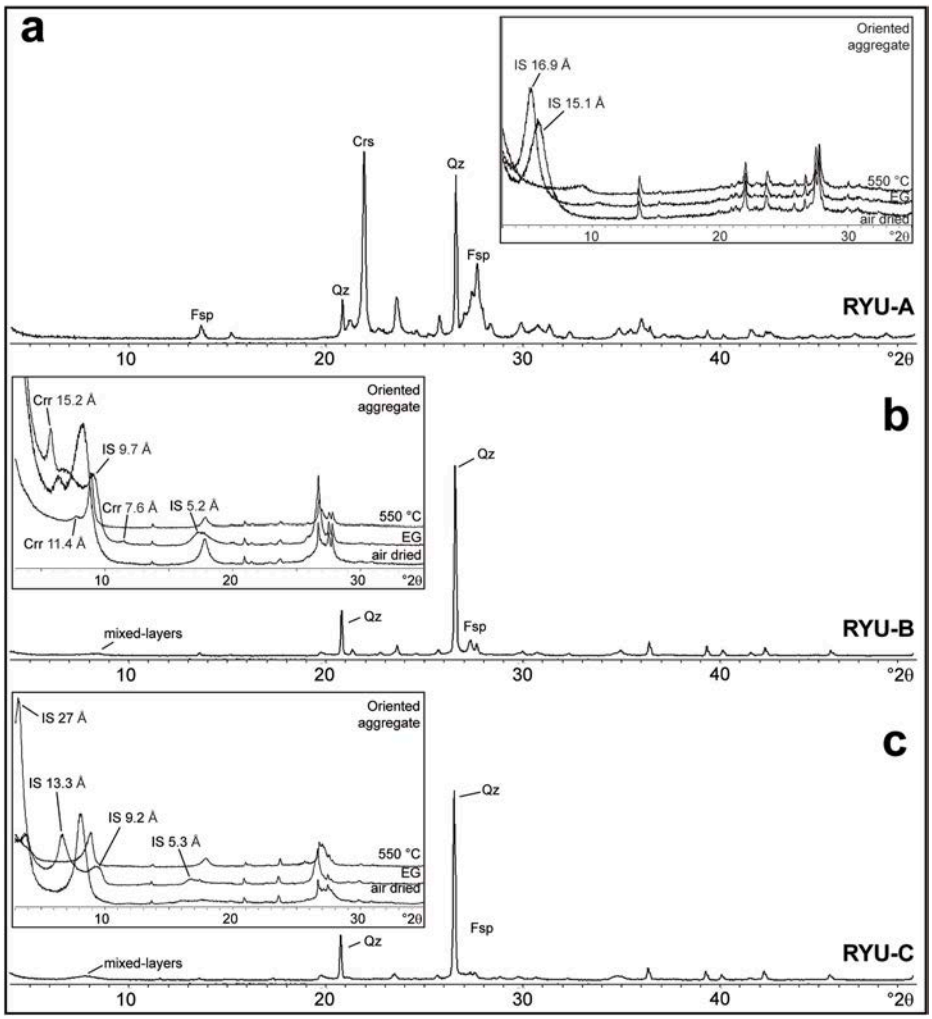

Fig. 3. XRD patterns for the analyzed raw materials. Bulk and oriented aggregates, air-dried, ethylene glycol solvated (EG), and heated to 550 °C of clay fraction (inset at the top left corner). (a) RYU-A,(b) RYU-B, (c) RYU-C. Abbreviations of minerals according to Whitney and Evans (2010): Qz, quartz; Fsp, feldspar; Crs, cristobalite; IS, illtite-smectite; Crr, corrensite.

stacking order R1. All identified phases are listed for each sample in Table 2.

Table 3 shows the weight losses (expressed Δwt.%) for bulk and finer clay samples, determined in thermogravimetry. As a whole, it is possible to observe three different thermal events. The first one (40–300 °C) is due to dehydration processes: water adsorbed at the surface of clay particle evolves below ~150 °C and the water molecules located in between clay slab and solvating cations are lost at higher temperatures [18]. Decomposition of ammonium ion takes place at ~450 °C [19]. The remaining effects are attributable to dehydroxylationat relatively low and high temperatures, namely within the thermal ranges 300–800 °C and 800–1000 °C [20]. Weight losses above 800 °C is due to the evolving of protons incorporated in the structure of tectosilicates [21]. In bulk clay samples (Fig. 4a) can be noticed the main occurrence of dehydroxylation between 300 and 800 °C, especially for IZU1, IZU2, RYU-B, and RYU-C. The latter sample (RYU-C) that contains a high amount of smectite displays the highest total weight loss (~4 wt%), along with a more evident dehydration under 300 °C and a dehydroxylation at higher temperatures. On the other hand, the weight losses observed in samples SHI2 and RYU-A that contain higher amount of non-plastic minerals are very low (Table 3). Comparing TG curves of bulk samples with those of the finer ones (Fig. 4b), it is possible to observe an increase of the weight losses calculated in the thermal ranges 40–300 °C and 300–800 °C as a consequence of an enrichment in clay minerals (Table 2). It is worthy to note the absence of the α-quartz → β-quartz polymorphic transition observable as the endothermic reaction at ca. 573 °C in the DSC measurements (not shown) of all examined samples. This aspect could due to the hydrothermal conditions suffered by raw materials.

According to FTIR results (Fig. 5, Table 4), dehydroxylation is due to the occurrence of 2:1 clays such as illite, testified by the absorption

Table 3
Weight loss (Δw%) of bulk and finer clay samples determined in thermogravimetry.

Bulk clay samples			
	40–300 °C	300–800 °C	800–1000 °C
SHI2	0.1	0.1	0
IZU1	0.2	1.3	0.2
IZU2	0.2	1.9	0.1
RYU-A	0.2	0.4	0.1
RYU-B	0.7	1.4	0.0
RYU-C	1.3	2.2	0.3
Finer clay samples			
	40–300 °C	300–800 °C	800–1000 °C
SHI2	0.6	0.9	0
IZU1	0.5	4.1	0.2
IZU2	0.3	4.8	0.2
RYU-A	2.9	2.1	0.1
RYU-B	1.4	3.6	0.1
RYU-C	2.4	4.1	0.7

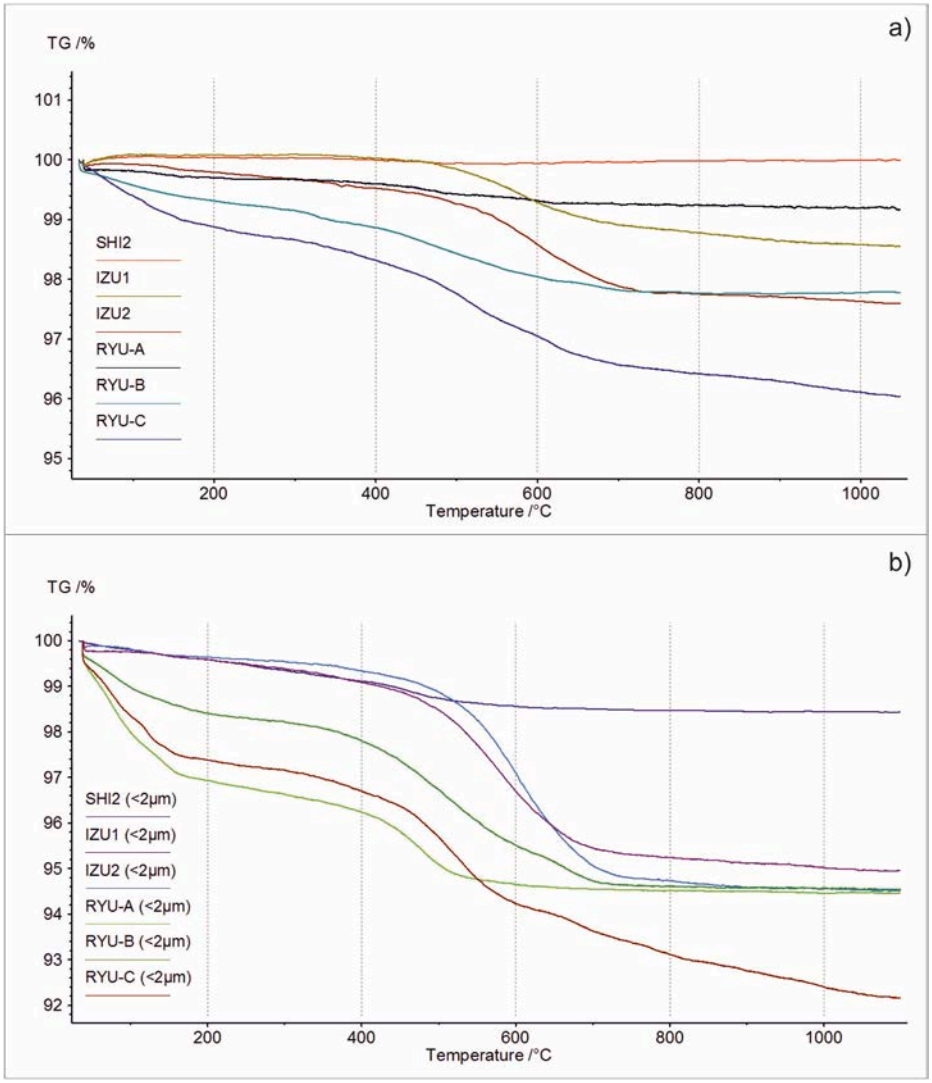

Fig. 4. TG curves of bulk (a) and finer (b) clay samples.

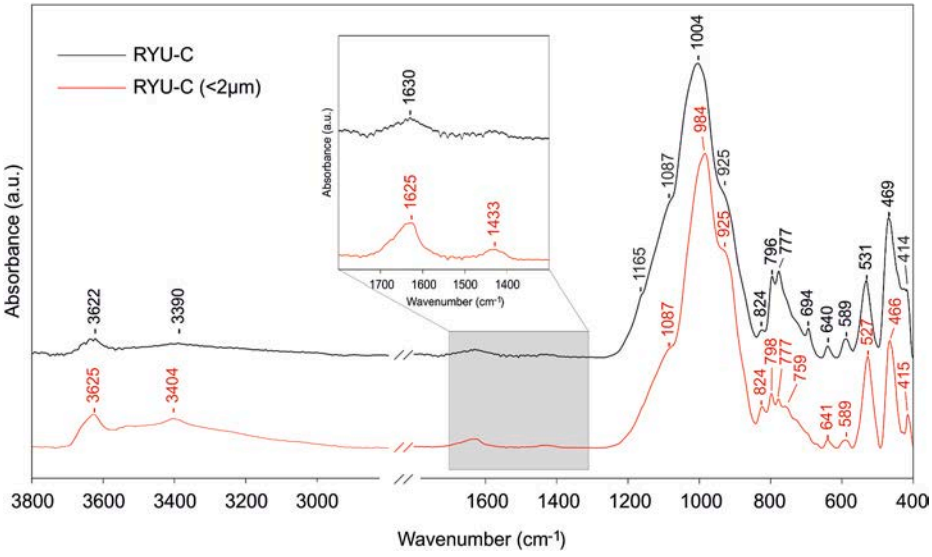

Fig. 5. Selected FTIR spectra of raw material (RYU-C).

Table 4
FTIR absorption bands (cm^{-1}) of raw materials. Note: w, weak; vw, very weak; s, strong; vs, very strong; br, broad; m, medium; sh, shoulder; T, tetrahedral site cations (Al or Si); M, monovalent and divalent cations; ν, stretching vibrations; δ, bending vibrations; γ, out-of-plane vibrations.

SHI2		IZU1		IZU2		RYU-A		RYU-B		RYU-C		Tentative of vibrational assignments	Chemical phases
bulk	<2 μm	bulk	<2 μm	bulk	<2 μm	bulk	<2 μm	bulk	<2 μm	bulk	<2 μm		
		3620 vw	3628 vw	3629 vw	3629 vw		3628 vw	3622 vw	3619 vw	3635 vw	3625 w	ν(O–H)	Illite
										3390 vw (br)	3405 w (br)	$\nu(H_2O)/\nu(NH_4)$	Illite/water
							1637 vw	1630 vw	1636 vw	1631 vw	1625 w	$\delta(H_2O)$	Illite/water
		1428 vw	1429 vw	1424 vw	1427 vw						1433 vw	δ(N–H)	Illite
		1162 sh	1164 sh	1163 sh	1162 sh			1164 sh	1163 sh	1165 sh	1165 sh	ν(Si–O)	Quartz
1092 sh	1090 sh	1089 sh	1062 sh	1088 sh	1062 sh	1095 sh	1089 sh	1091 sh	1085 sh	1087 sh	1087 sh	ν(Si–O)	Quartz
1004 vs	1000 vs	1008 vs	991 vs	993 vs	984 vs	1011 vs	998 vs	1001 vs	986 vs	1004 vs	984 vs	ν(T-O)	Illite/Feldspars
		932 sh	932 sh	934 sh	929 sh						925 sh	$\delta(Al_2OH)$	Illite
		831 vw	828 vw	829 vw	827 vw				824 vw	824 vw	824 vw	γ(Al–O)/δ(AlMgOH)	Illite
799 sh	797 m	796 s	799 sh	796 s	799 w	797 w	795 w	795 s	798 w	796 m	798 w	ν(Si–O)	Quartz
778 m	778 m	777 s	779 m	776 s	779 w	777 w	781 vw	777 s	779 w	777 m	778 w	δ(Si–O)	Quartz
760 sh	763 sh		755 sh		754 w						759 sh	δ(Al–O–Si)	Illite/Feldspars
694 sh	694 sh	694 m	696 m	694 m	695 w			694 m	696 vw	694 w		δ(Si–O)	Quartz
645 m	645 m	641 vw	642 vw	628 vw	626 vw	640 w	641 vw	641 w	642 vw	640 vw	641 vw	δ(T-O-T)/ν(M − O)	Illite/Feldspars/ Quartz
586 s	585 s	588 vw	585 vw		579 vw	583 m	582 m	588 w	588 w	589 w	589 vw		
539 m	540 m	531 m	531 m	531 s	528 s	546 w	545 w	533 m	529 m	531 m	527 m		
465 w	466 w	462 s	466 s	465 s	464 s	471 w	471 w	464 s	464 m	469 s	466 m		
425 m	426 m		428 w			424 m	421 w	425 sh	423 m				
			416 w		411 vw			412 vw		414 vw	414 w		

bands located between 3620 and 3637 cm^{-1} (OH vibrations) as well as the strong band at around 1000 cm^{-1}(Si–O asymmetric stretching mode) and a medium one at around 694 cm^{-1}. The presence of broad, weak absorption bands at ca. 3400 and 1631 cm^{-1} account for the occurrence of interlayer water, typical of smectite (samples RYU-B and RYU-C) plus potential contribution of ammonium ions.

Absorption peaks at 795 cm^{-1} and 777 cm^{-1} (samples RYU-B, RYU-C, IZU1, IZU2), along with the peak at ca. 694 cm^{-1} and the shoulder at 1662-1663 cm^{-1}, deal with the diagnostic doublet indicating the presence of quartz. This doublet seems to be less evident in sample RYU-A, whereas the peak at ca. 694 cm^{-1} disappears and the shoulder slightly shifts to higher wavenumber (ca. 1095 cm^{-1}). These features could be indicative of the occurrence of a high-temperature silica polymorph (e.g., cristobalite). It is worth noting here the occurrence of the bands 1428 cm^{-1}, 1427 cm^{-1} and 1433 cm^{-1} for samples IZU1, IZU2 and RYU-C respectively: according to literature [19], these bands suggest the partial replacing of K^+ with NH_4^+ in illite.

4.1.2. *Chemical characteristics of raw materials by XRF analysis*

XRF compositions are shown in the bivariate plots in Fig. 6. Ryumon and Shirakawa clays are characterized by lower counts of Si and Al. Izumiyama clay is illitic in nature and features an appreciable presence of kaolinite that increases the Al content and the refractoriness. Potassium content is rather similar in all the samples, except some Ryumon ones that exhibit lower values. XRF compositions prove perfectly consistent with XRD results as the kaolinite-lacking and interstratified clay-type from Ryumon deposit, contrary to Izumiyama highly illitic clay, bears variable illite-smectite relative contents and significant presence of remnant alkali-feldspars (Sanidine/Orthoclase) and sodic feldspars (Plagioclase). Shirakawa consists of quartz and plagioclase with no phyllosilicate minerals. The segregation between Izumiyama and the other clays in the Si–Al and Si–K bivariate plots (Fig. 6) is obvious.

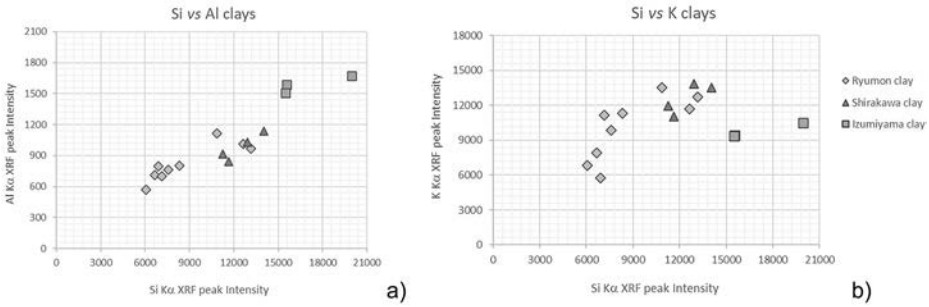

Fig. 6. Bivariate plots of clay groups based on Si–Al (a) and Si–K (b) Kα signal intensity detected in the samples analyzed by XRF analysis.

4.2. Shards - chemical composition and elemental correlation in porcelain bodies

The Si–Al plot in Fig. 7a clearly shows a linear trend toward higher contents of Si and Al in raw materials used for porcelain bodies. The variation of K is limited (Fig. 7b) and Ca amounts are low, except for rare outliers (Fig. 7c). The chemical composition is consistent with the firing of an illitic clay: the high amount of K is the result of the alteration process of potassic feldspar (orthoclase or sanidine) with subsequent formation of illite, while the low amount of Ca (and Mg) is related to a small presence of smectite, the mineral mainly produced by the alteration process of plagioclase. The amount of smectite (montmorillonite) in the illite and illite-kaolinite alteration zones is very low as confirmed by the data presented in Table 2. Therefore the best clay appears to have come from the Izumiyama deposit, where, as we have seen in section 2.1, the most desirable grade consisted of pure illite, which is mainly present in the two highly altered zones of the deposit.

A noticeable variability characterizes the contents of K and Ca in some of the bodies, especially those produced between 1610 and 1630 (Fig. 8). A larger amount of calcium is measured. These findings indicate that the clay used in the earliest production period had been indistinctly extracted (and possibly mixed) from different alteration zones of Ryumon deposit. As we have established in the previous section, porcelain stones sourced from the weakly altered zones feature significant amounts of remnant feldspars and smectite. Therefore, a chemical composition richer both in K and Ca, or richer in Ca and poorer in K, implies that residual alkali-feldspars and/or alteration products of feldspars such as smectite characterize the raw materials used for body production.

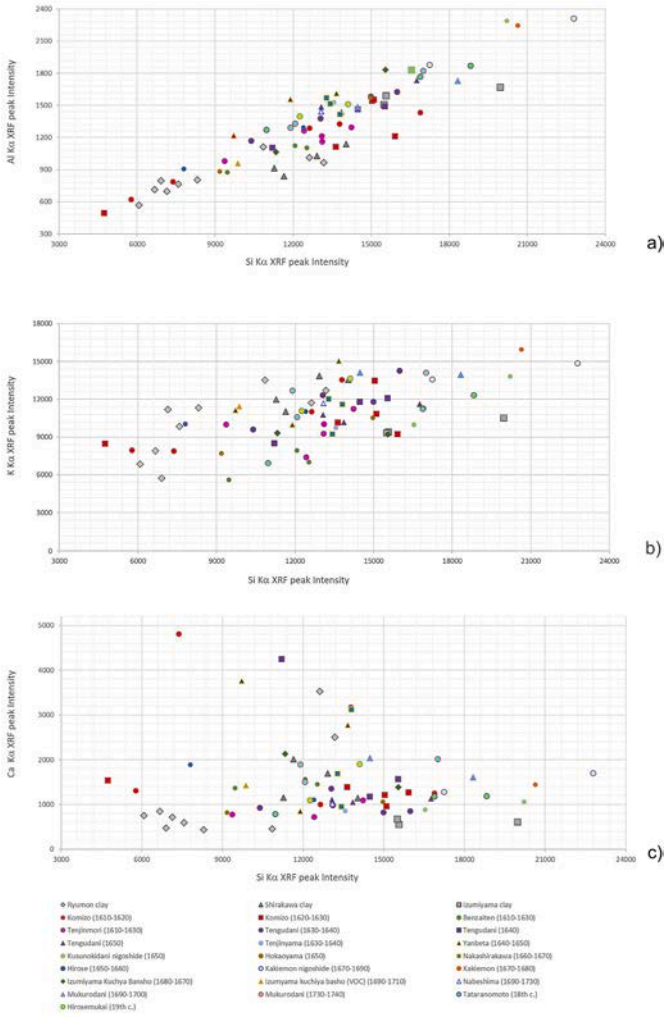

Fig. 7. Bivariate plots of a) Si–Al, b) Si–K, c) Si–Ca for the analyzed shards' bodies and clays.

Analytical evidence points to a gradual improvement in material selection and processing. Such an improvement became more evident when the use of Izumiyama clay started in the 1630s. Clusters of shards that group around Ryumon clay confirm that the deposit was exploited before the 1630s for body-making until the discovery of the Izumiyama quarry as testified by the shards excavated from Tengudani kiln in 1630–1640. Shirakawa deposit appears to have been exploited (and possibly discovered) in the mid-to-late 1620s and mostly reserved for glaze-making in consideration of the non-clay nature of its constituent minerals.

Most of the bodies are also characterized by high amounts of Rb and low amounts of Sr. Strontium and Rubidium are common trace elements associated respectively to calcium (Fig. 9) and potassium. The relative amounts differ usually in relation with orogenesis and are commonly used in archaeometry to differentiate raw materials origin. Generally, Sr substitutes for Ca and Rb substitutes for K [22,23], illitic clay is a fine grained mineral that contains low amounts of Ca, therefore the results are perfectly consistent with the expected chemical composition of a highly altered clay used for making the bodies. It is interesting to note here that some correlation between Ca and Sr can be identified in some of the clays and bodies analyzed. Ryumon clay and shards from the early Komizo kiln, located to the far right of the plot in Fig. 9, show correlation between Sr and Ca. Since it is well known that rhyolites can exhibit covariance between those two elements [22,23], not only are the findings perfectly consistent with the origin of Ryumon clay (hydrothermally altered rhyolite), but they also suggest that such clay, mixed or unmixed, must have been used for body production at the early kilns of Arita, especially between 1610 and 1630, and that the practice of mixing clays from different alteration zones marked Japanese porcelain production throughout the Edo period (1603–1868) as Yanbeta (1640s) and later shards seem to indicate (see section 4.4).

This last analytical evidence confirms that the kilns lacking official patronage such as Komizo and later Yanbeta, located in the Sotoyama area in the western part of Arita, mostly used lower grades of clay, contrary to the kilns strictly controlled by the Nabeshima clan, located in the Uchiyama area, which were supplied with better grades.

We can conclude that, whenever possible, raw materials extracted from highly altered zones were preferred for making high-grade porcelain bodies, especially after the 1630s, while clays indistinctly extracted, and possibly mixed, from different alteration zones appear to have been employed for making most of the bodies before 1630s, and even some export wares destined to Europe in the late 17th and early 18th centuries (shard from Izumiyam Kuchiya Bansho site with VOC lettering). The practice of employing different grades of materials for distinct porcelain productions is also confirmed by recent systematic studies on Japanese enamels for overglaze decoration [5,6]. Moreover, clusters of shards that overlap in the middle section of the Si–Al bivariate plot (Fig. 7a) suggest again that different grades of clay were mixed throughout the Edo period, considering that mixing different clays is a common factory practice aimed at optimizing the rheological and mechanical properties of the paste and of the green body as well the profile of the shrinkage [18]. Furthermore, mixing was also a consequence of the strict control by the authorities on clay quality and supply.

The production method and materials identified so far are further confirmed by our analysis of a Chinese Shonzui-style (1630–1640) underglaze-blue-decorated shard excavated at Yanbeta kiln site (Fig. 10). The discovery of this shard is extremely important as it firmly proves, for the first time, that imported Chinese porcelains were actually present at kiln sites in Arita in the 1630s. This crucial instance enables a deeper understanding of the first phase of porcelain production in Japan as it confirms that both Chinese books and imported porcelains fired at Jingdezhen (China) served as models for early-stage design

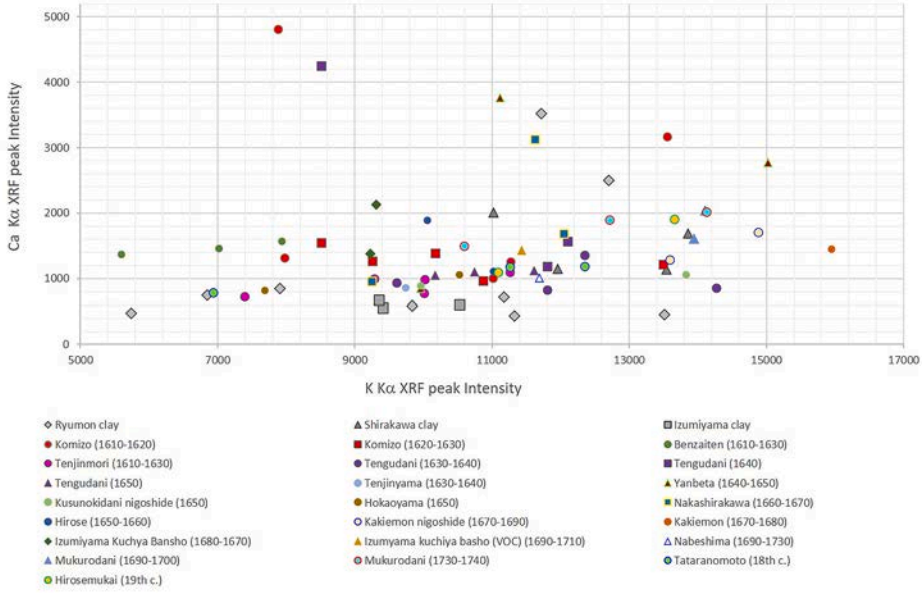

Fig. 8. Bivariate plot of K–Ca for the analyzed shards' bodies and clays.

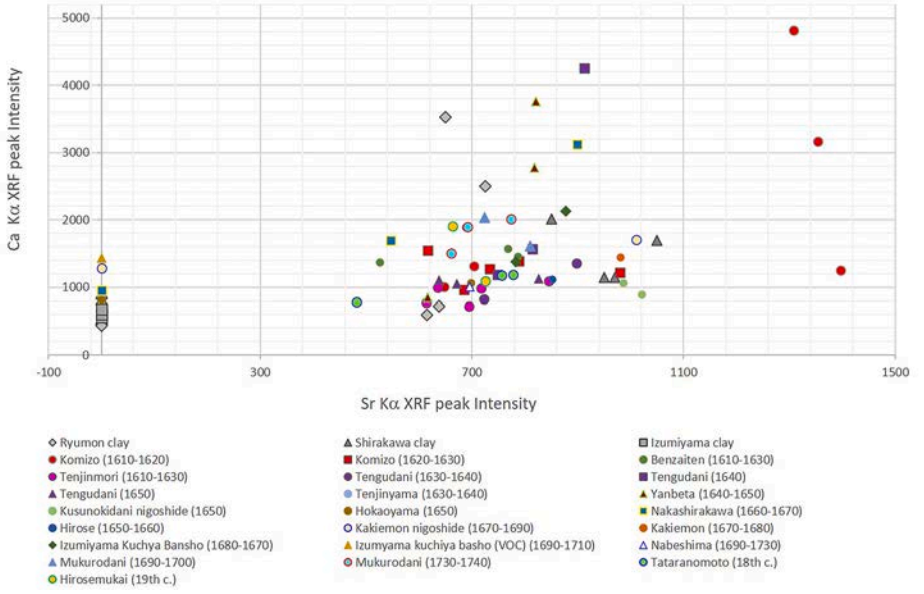

Fig. 9. Bivariate plot of Sr–Ca for the analyzed shards' bodies and clays.

Fig. 10. Shonzui-style shard (1630–1640), Jingdezhen, China, excavated at Yanbeta kiln site.

development. This suggests that also highly expensive Chinese white wares, being of a much better grade than Japanese ones at the time, had most likely been sparingly imported to be used for the earliest experimentation with overglaze enamels under the supervision of Europeans as detected in a previous work [5–7].

According to its style, the porcelain cup (Fig. 10) was fired at Jingdezhen, in the late Ming period (1630–1640) and it served as a model to Japanese potters. The Si–Al plot for the body (Fig. 11) unquestionably shows that its composition differs completely from the Japanese recipe. The Jingdezhen shard bears a much higher Al content as expected with the use of kaolin that characterizes the Chinese recipe for body production [14,24]. Moreover, the content of Si appears to be clearly in line with the type of clay, richer in alkali-feldspars and therefore located in the mid-part of the bivariate plot, that has been identified to have been used at Jingdezhen after the introduction of the porcelain stone-kaolinite recipe in the 14th century [14,24]: such clay could only have been extracted from weakly altered zones where remnant alkali-feldspars are significantly present. Therefore the Si content of the analyzed Chinese body further confirms that most of Japanese shards, as demonstrated so far, were made using a mixture of clays sourced from different alteration zones.

4.3. Shards - chemical composition and elemental correlation in porcelain glaze

The evident linear trend in the Si–Al plot reported in Fig. 12a shows the nature of the glazes produced at Arita kilns during the Edo period. Clays for glaze-making were basically sourced from the weakly alteration zones of the deposits available at the time of production as the melting temperature had to be kept lower than that of the bodies in order to avoid deformation during the firing process. Materials extracted from such zones would contain higher amounts of fluxing agents such as alkali-feldspars and/or flux-rich products of the hydrothermal alteration process and low amount of illite and kaolinite or no kaolinite at all.

The complete segregation of the clays extracted from the illite/illite-kaolinite zones of the Izumiyama deposit firmly indicates that such high-grade clays were not used as glazing materials due to both their limited availability and their low flux content.

The results displayed in Fig. 12 confirm that Japanese potters employed porcelain stone and wood ash as glaze ingredients: the complete segregation between the chemical composition of the clays (far bottom) and the shards, especially their different Ca (Fig. 12b) and Sr (Fig. 12c) contents, firmly points to a mix of porcelain stone and botanic ash. Botanic ash brings the high contributions of Sr and Ca [25], elements which are very low in the porcelain stone used for the bodies, as shown in the plots. It is known that botanic ash in Arita, rich in Sr and Ca, comes from *Distylium racemosum* (*isunoki*), a characteristic tree that abundantly grows in Kyushu and that was used as the chief material from which wood ash was obtained for glaze production in Arita [26,27]. Therefore, we can definitely conclude that Japanese tradition was basically influenced by Korean technology: porcelain stone for the bodies, and a mix of porcelain stone and wood ash for the glaze. These compositions differed dramatically from Chinese ones, and they also show that even when new potting techniques were introduced in Arita by Chinese potters in the 1640s for the development of better-grade bodies suitable for overglaze enameling, Japanese potters remained loyal to the first Korean technological influence which had led to the development of porcelain bodies and glazes in Japan in the 1610s [3,4].

4.4. Comparison with Korean and Chinese glazing technologies

The Si–Ca and Sr–Ca bivariate plots in Fig. 12b and c provide the definitive scientific evidence that porcelain glazing technology developed in Japan on the basis of Korean ceramic tradition, and that this practice remained completely separated from the Chinese production methods employed at Jingdezhen. Porcelain production in Arita owes its birth to the Korean potters who settled in Kyushu, the southernmost island of the Japanese archipelago, in the Momoyama period (late 1590s). In particular, *punch'ŏng* wares played a major role in the technological transfer as potters involved in their production were taken to Japan by Toyotomi Hideyoshi after the two Korean military campaigns (1592–98) [15]. The movement of such a significant number of potters is believed to have partly caused *punch'ŏng* production to cease entirely in the late 1590s [15]. Recent studies have confirmed that the body of *punch'ŏng* wares consisted of kaolinized porcelain stone similar in composition to Japanese clay [15,24] and therefore completely different from the porcelain stone-kaolinite mix of Chinese origin. Korean glazing technology was instead characterized by the employment of two different mixtures of materials: a first recipe based on porcelain stone, glaze ash (main flux ingredient) and wood ash, influenced by Chinese tradition (from the 14th century) [15], and a second recipe based on porcelain stone mixed with wood ash as the chief flux ingredient,

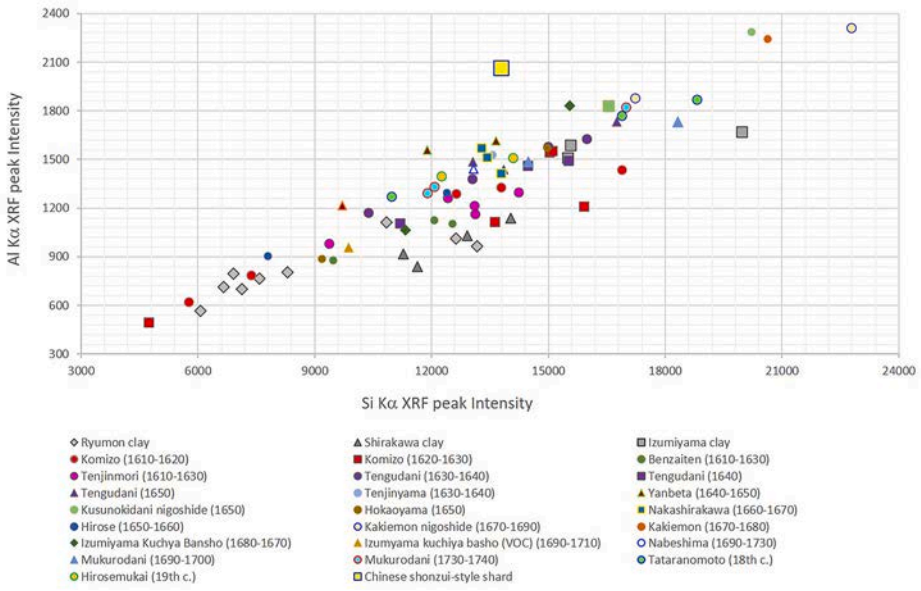

Fig. 11. Bivariate plot of Si–Al for Japanese and Chinese porcelain shards' bodies and clays.

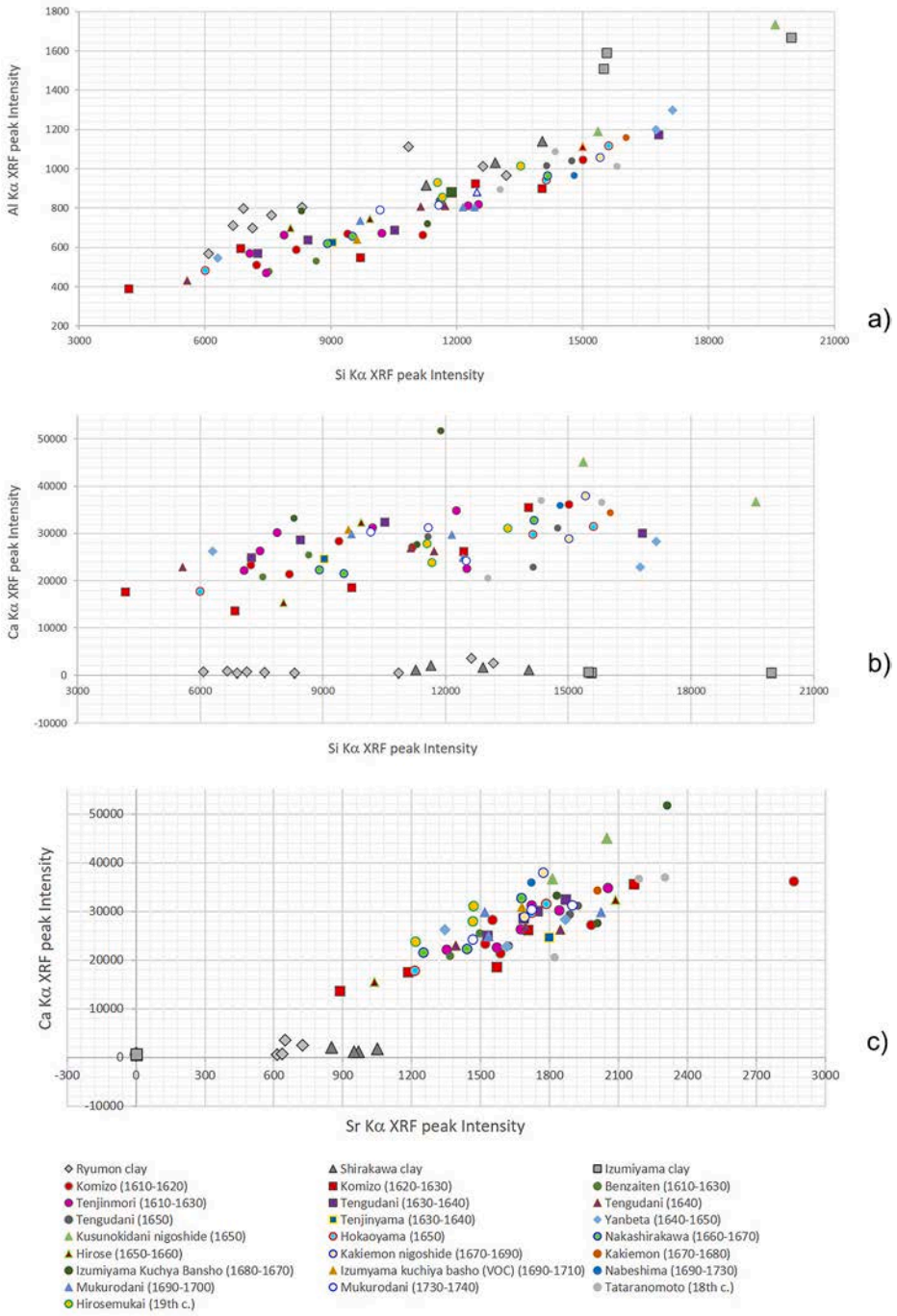

Fig. 12. Bivariate plot of a) Si–Al, b) Si–Ca, c) Sr–Ca for the analyzed shards' glaze and clays.

consistent with the Koryŏ tradition [15].

The technological difference that marked Chinese and Japanese productions also emerges from the plot in Fig. 13. As expected, the glaze on the Jingdezhen shard (see section 4.2) does not belong to the group of Arita glazes. The content of Ca and Sr firmly indicates that the Chinese used porcelain stone, glaze ash and a much smaller amount of wood ash, contrary to Japanese practice that was based on the use of porcelain stone and botanic ash as the main fluxing ingredient. Once again XRF analysis has provided crucial evidence to learn more about the production process and the materials employed in Japan and their difference with the Chinese tradition.

4.5. *The development of porcelain bodies in the early kilns (1610–1650): Komizo and Tengudani*

The development of porcelain bodies started in western Arita in the 1610s with potters aiming at gradually improving the overall physical properties of the wares through tireless experimentation. Komizo kiln operated between 1610 and 1630: it was then shut down in the early 1630s to establish the Tengudani kiln right after the discovery of the Izumiyama clay deposit [3,4]. We will now focus the attention on these kilns: the bivariate plot in Fig. 14 shows the Si and Al contents as detected on the shards excavated from Komizo and Tengudani (Table 2).

The distribution of the shards in the plot clearly illustrates a gradual improvement in material selection and processing as experimentation

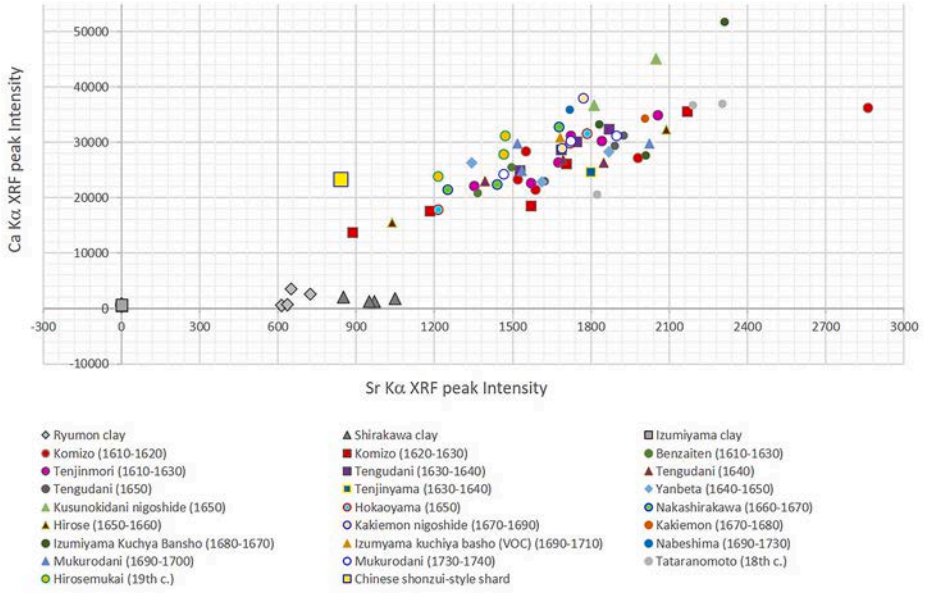

Fig. 13. Bivariate plots of Sr–Ca for the Japanese and Chinese shards' glaze and clays.

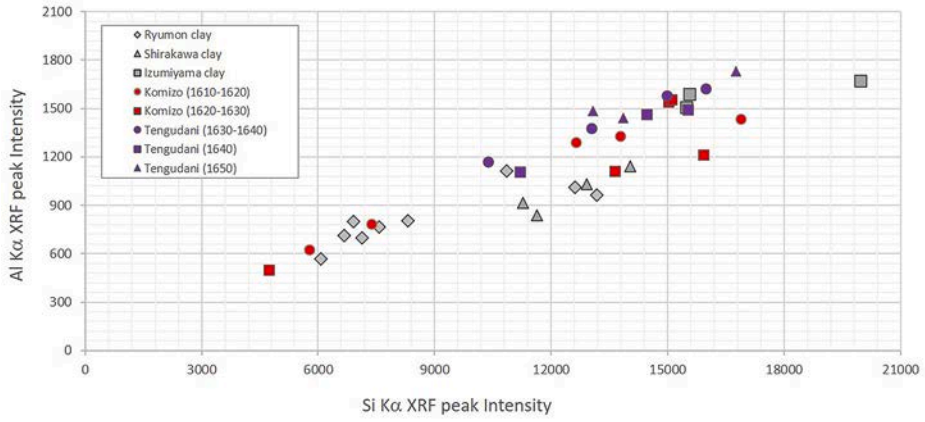

Fig. 14. Bivariate plot of Si–Al for the analyzed shards' bodies excavated at Komizo and Tengudani kiln sites and clays.

with clays proceeded from the 1610s. Komizo shards, mostly located in the bottom-left and central part of the bivariate plot, well overlap with the composition of the kaolinite-lacking and interstratified illite-smectite clay-type sourced from Ryumon deposit. Tengudani shards, instead, are characterized by a higher Al content owed to an appreciable presence of illite and kaolinite in basically all Izumiyama alteration zones: they mostly group in the upper right part of the bivariate plot, thus segregating from the average Komizo composition. Tengudani shards distribution indicates that a stabilization of production was reached in the late 1630s to early 1640s, and that similar clays were used throughout the 1640s and up to the early 1650s as shown by the shards that surround Izumiyama clay samples (illite-kaolinte alteration zone). The last period of Tengudani production (early1650s), represented here by the lone shard (triangular-shaped violet color) located in the far upper-right of the bivariate plot, where the pure illitic Izumiyama clay sample lies, testifies that after a steady use of clays sourced from the alteration zones illite-kaolinite and weakly altered I, a partial exploitation of the limited illite zone of the Izumiyama deposit started in the early 1650s. This circumstance remarkably matches the contemporary employment of Izumiyama pure illitic clay for the development of the *nigoshide* (milky-white) body at Kusunokidani kiln in 1650 (see section 4.7). Those instances point to the early 1650s as the period marking the first ever exploitation of the illite zone of the Izumiyama deposit, most likely through a progressive digging from the surface rich in feldspar toward the center rich in illite [12]. It appears clear now how this newly available high-quality clay triggered a stricter control on the limited resource by the Nabeshima clan, who granted its supply to distinguished potters as testified by the Kusunokidani and Kakiemon nigoshide-body compositions (see section 4.7), and by the Kakiemon blue-and-white shard located in the upper right of the Si–Al bivariate plot (Fig. 7a). The Si–Al bivariate plot (Fig. 7a) also shows that the 18th and 19th centuries will be characterized by the use of heterogeneous clay qualities, and that likely a mix of different clay grades from Izumiyama alteration zones was the main material available for body production [1].

It is relevant to note here (Fig. 14) that in the late period of Komizo operations (late 1620s to early 1630s) potters laid the foundation for porcelain production at the to-be-newly-established Tengudani kiln. Komizo shards fired from the mid-to-late 1620s group in the middle area of the Si–Al bivariate plot (Fig. 14), suggesting that the constantly improving material selection and processing were actually limited by the kaolinite-lacking and interstratified nature (illite-smectite) (Table 3) of the clay sourced from Ryumon deposit. The two Komizo shards (1620–1630) that homogeneously group in the upper-right section of

the Si–Al bivariate plot (Fig. 14) testify to the use of a clay-type similar to RYU-B (interstratified 80% illite - 20% smectite), which must have become available, on a very limited basis, by the late 1620s to the early 1630s at Ryumon deposit.

A broader use of clays sourced from the illite-kaolinite and illite alteration zones of the Izumiyama deposit will enable a steadier production of better porcelain bodies from the mid-to-late 1640s at kilns such as Tengudani.

The XRF bivariate plots, therefore, along with XRD mineralogical analysis, enable the identification of the materials used in the early period of porcelain production in Arita, and allow for the tracing of the different phases that characterized material selection and processing at a given time for a specific kiln. They also enable a clear distinction between potters' choices in terms of material use for different productions, that is, domestic and export, throughout the Edo period (Fig. 7).

To conclude, analytical evidence suggests that a kaolinite-lacking and interstratified illite-smectite type of clay sourced from Ryumon deposit was mainly used during the earliest phase of porcelain experimentation and production (1610–1630) at kilns located in western Arita (Komizo, Tenjinmori, Benzaiten, etc). The very limited availability of a highly altered clay-type at Ryumon deposit, along with its inconvenient location and the long-hypothesized presence of arsenic [1], confirmed by our XRF analysis for the first time (Fig. 15a), led to its abandonment by most potters (see following section) in the early 1630s right after the discovery of Izumiyama deposit. In particular, the high presence of As detected on Ryumon clay-samples appears to suggest that the hydrothermal alteration process of Ryumon rhyolite occurred at a lower temperature compared to Izumiyama deposit [28]: the kaolinite-lacking and interstratified (illite-semctite) nature of the clay; the high Fe content (Fig. 15a) and its favorable effect on As-adsorption by the smectitic component (montmorillonite) at lower temperatures [29,30]; along with the As-adsorption dependence on pH variability [28–31], all consistently point to a lower-temperature hydrothermal alteration process and a likely different fluid composition/hydrothermal system. Not to be ruled out is also the possibility that a contribution to the whiteness of the bodies may have come from the precipitation of the arsenic-based phase(s).

The use of porcelain stone mostly sourced from the outer alteration zones of Izumiyama deposit, characterized by a higher Al content compared to Ryumon clay, appears to have started at Tengudani in the early 1630s. The 1640s are characterized by an overall improvement in material selection and processing as well as a consistent employment of clays sourced from the illite-kaolinite alteration zone. The early 1650s will see the first exploitation of the limited illite alteration zone of Izumiyama. Such pure illitic clay will enable the development of iconic porcelain wares that will take Europe by storm in the second half of the 17th century. Evidence shows that the clay-types sourced from the weakly altered zones of Izumiyama deposit will mostly be used from the second half of the 18th century, when it is likely that the illite-kaolinite and illite zones were nearing depletion. Moreover, mass-produced and export wares appear to have generally consisted of lower-grade bodies, and consistently group in the middle and lower-left of the bivariate plot (Fig. 7), thus testifying to the high variability of the materials available to potters in terms of overall quality.

Further evidence comes from the SEM-EDS quantitative microchemical analyses performed on shards of porcelain bodies selected from different kilns and periods: lower Al_2O_3 concentration in bodies from the early kilns is confirmed, as well as an increase in Al_2O_3 concentration in porcelains produced in later periods (Table 5).

4.6. Ryumon clay and the Sotoyama kilns: mass production at Hirose after the 1630s

Shards fired in the mid-17th-century at Hirose kiln, located in the Sotoyama (western) area of Arita (very close to Ryumon deposit), group at the bottom-left and central part of the Si–Al bivariate plot (Fig. 7a) together with the kaolinite-lacking and interstratified illite-semctite clay-type sourced from Ryumon deposit. Arsenic was detected in both the glaze and body of such mass-produced wares (Fig. 16 a,b,c).

This first-time-ever discovery clearly reveals that potters kept using cheaper clay sourced from Ryumon at least until the late 1650s in order to lower firing temperatures and cut on production costs. The appreciable presence of arsenic in the analyzed shards implies that high-firing was carried out at a lower temperature than the standard 1270 °C–1300 °C, during which volatile As was lost (position of wares in kiln

Table 5
Representative samples for the different kilns and periods in relation to their Al_2O_3 concentration (average of five areas for sample) analyzed via SEM-EDS microanalysis.

SHARD	KILN	PERIOD OF PRODUCTION	QUANTITATIVE DATA % Al_2O_3
EARLIEST KILNS IN SOTOYAMA AREA (WESTERN ARITA) 1610–1630 Al_2O_3% [15-17%]			
1C	KOMIZO	1610–1620	**16.57**
2B	KOMIZO	1620–1630	**15.98**
3C	TENJINMORI	1610–1630	**17.83**
KILNS IN UCHIYAMA AREA (EASTERN ARITA) 1630s - 19th CENTURY Al % [17-22%]			
4C	TENGUDANI	1630–1640	**18.16**
5A	TENGUDANI	1640	**17.25**
5C			**19.36**
6C	TENGUDANI	1650	**19.28**
7B	HOKAOYAMA	1650	**16.94**
8B	NAKASHIRAKAWA	1660–1670	**19.52**
9C	IZUMIYAMA KUCHIYA BANSHO	1680–1690	**17.36**
10A	MUKURODANI	1690–1700	**21.66**
10B			**19.48**
11B	MUKURODANI	1730–1740	**18.82**
12A	TATARANOMOTO	18 TH CENTURY	**22.52**
13A	HIROSEMUKAI	19 TH CENTURY	**19.15**

Areas of polished samples measured via SEM-EDS and EDS analyses are available in the Supplementary files.

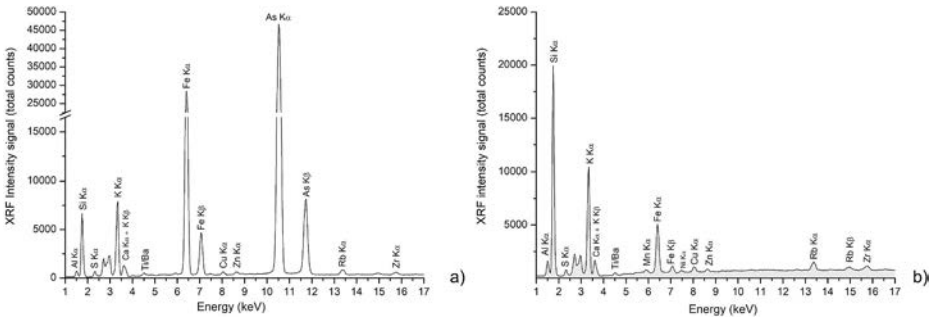

Fig. 15. (a) XRF spectrum of Ryumon clay showing high contents of As and Fe; (b) XRF spectrum of Izumiyama clay showing lower Fe content and no As.

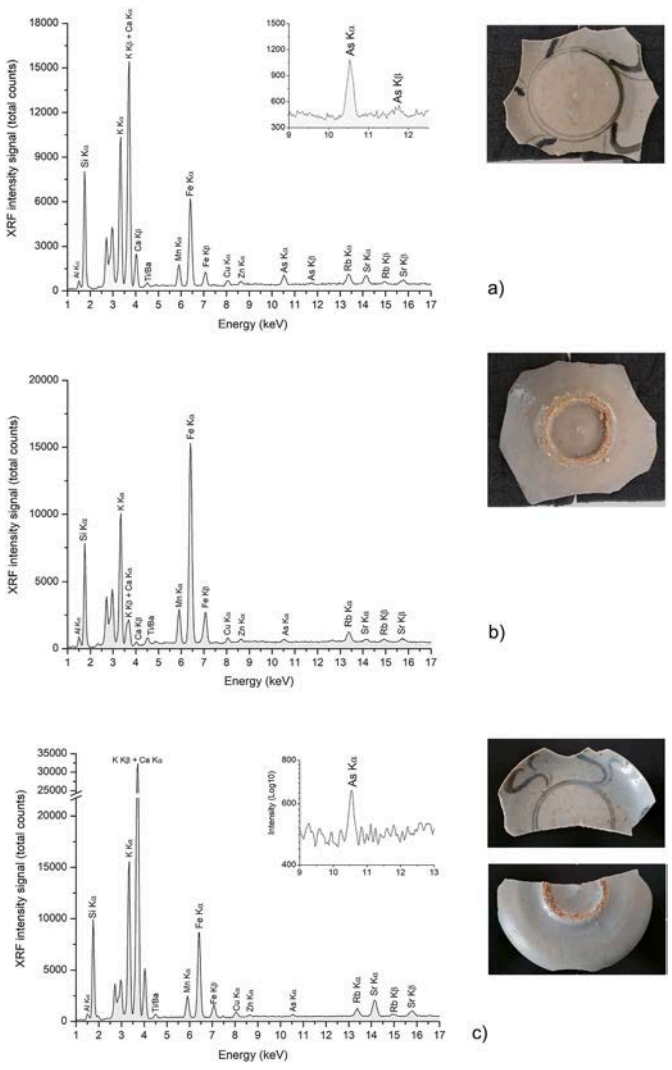

Fig. 16. XRF spectra of the analyzed shards excavated at Hirose kiln site (1650–1660) showing an appreciable presence of As: (a) glaze, (b) body, (c) glaze.

chambers proved therefore crucial), and that clay had to be characterized by a very high arsenic content as consistently observed in the composition of the analyzed raw material from Ryumon deposit (Fig. 15a). The scientific evidence confirms that kilns in the Sotoyama area did not benefit from the Nabeshima patronage as the Uchiyama (eastern area of Arita, closer to Izumiyama deposit and strictly controlled by the Authorities) kilns did, and that potters, in order to survive, needed to come up with ways to mass-produce porcelains that would appeal to the lower-end of the domestic market: cutting on production costs became a matter of survival, and the use of low-grade Ryumon clay (Type C: interstratified Illite-Smectite, 60% illite - 40% smectite, with high As content, Fig. 15a, Table 2; or Type B: interstratified illite-smectite, 10% illite - 90% smectite) (Table 2) to improve profits became mandatory, considering that a *Noborigama* (chambered climbing) kiln was a very expensive piece of equipment to manage [1].

To conclude, the scientific evidence herein presented strongly points to the low-grade kaolinite-lacking and interstratified illite-smectite clay-type sourced from Ryumon deposit as the cause of the significant number of collapsed wares (Fig. 17) that characterized mass production at Hirose kiln in the 1650s.

4.7. *The development of the nigoshide body*

It is highly relevant to focus here on the development of the famous *nigoshide* (milky-white) body. *The nigoshide* body, characterized by its pure white color, marked the production of the renowned Kakiemon wares, mostly fired in their classic forms and decorations between 1670s and 1690s [27,32].

It has recently been confirmed that Kakiemon I (1586–1666) worked at Kusunokidani kiln [32] before moving to Nangawara for the establishment of his own kiln around 1660. In particular, excavations at Kusunokidani kiln site led to the discovery of a kiln utensil inscribed with the name Toshikiyama, used at the time to indicate the area where the kiln was located (close to the Izumiyama deposit) [32]. The same name Toshikiyama had also been mentioned in one of the documents in possession of the Kakiemon family as the place where Kakiemon had initially worked before founding his own kiln [32].

In terms of scientific evidence, we have analyzed the very scarce *nigoshide* shards excavated at the Kusunokidani and Kakiemon kiln sites (Table 6) by EDXRF (non-destructive analysis was mandatory).

The bivariate plot reported in Fig. 18 offers clear evidence of the similar origin of the two bodies. Both Kusunokidani and Kakiemon shards group to the top-right of the bivariate plot(s), indicating their close relation to the best-grade Izumiyama clays extracted from the illite-kaolinite and illite zones, along with a more efficient processing method. These findings confirm the discovery of Izumiyama deposit around the 1630s [3,4] and the probable exploitation of its pure illitic zone starting from the early 1650s, as no other clay deposits, namely Ryumon and Shirakawa, appear to have been characterized by the same

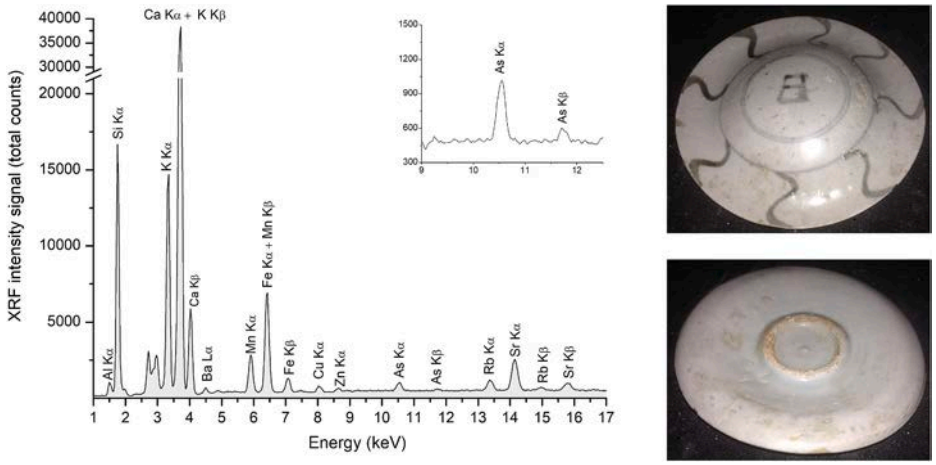

Fig. 17. XRF spectrum showing the presence of As in the glaze of a collapsed dish (1650–1660) fired at Hirose kiln.

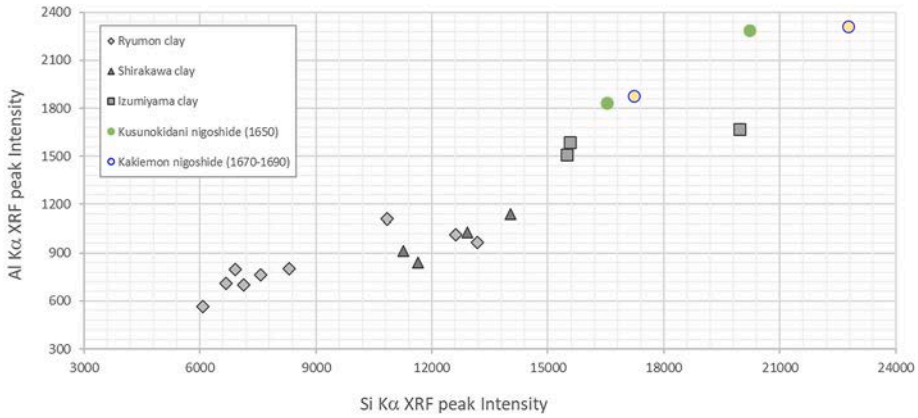

Fig. 18. Bivariate plot of Si–Al for the analyzed nigoshide shards excavated at Kusunokidani and Kakiemon kiln sites and clays.

Table 6
Analyzed nigoshide-white bodies excavated at Kusunokidani and Kakiemon kiln-sites.

Kiln site	Sample	Period of production	Technology
Kusunokidani	**n. 412**	1650	
	n. 431	1650	
Kakiemon	**n. 43_1**	1670–1690	
	n. 731	1670–1690	

clay compositions. Furthermore, it is evident that the best-grade Izumiyama clay was made available by the authorities to potters at Kusunokidani as testified by the shards' chemical compositions. In regard to the Kakiemon nigoshide body, results indicate that it bears Si and Al contents comparable to the Kusunokindani one. It has to be considered that some variability is expected as far as the levigation process is concerned, especially due to a certain degree of inhomogeneity that may characterize the clays even when extracted from the same alteration zones. To conclude, analytic evidence suggests that the recipe used to create the first *nigoshide* body at Kusunokidani kiln around the 1650s was later employed by Kakiemon to produce the same kind of porcelain body from the 1670s at Nangawara. Thus science strongly points to the involvement of Kakiemon I in the development of the first nigoshide body at Kusunokidani kiln. The production then continued at the Kakiemon kiln, suggesting that the inception of such a high-grade body may have been the result of Kakiemon's own intuition and effort.

5. Conclusions

Analytic evidence confirms that porcelain production started in western Arita in the 1610s at Komizo kiln after the discovery of hydrothermally altered rhyolite at Ryumon deposit. Material processing and clay selection improved gradually on the basis of an extensive experimentation with the kaolinite-free and interstratified-illite-smectite clay-type sourced from Ryumon. Bodies fired in the earliest period (1610–1630) feature, on average, lower contents of Si and Al, hence a lower firing temperature, while wares fired after the discovery of hydrothermally altered rhyolite at Izumiyama deposit, richer in illite and containing kaolinite, are characterized by a consistently higher presence of Al and Si as testified by the porcelains fired at Tengudani kiln from the early 1630s. Ryumon deposit will be abandoned by most potters in the early 1630s, yet the use of its clay appears to have continued for the mass-production of wares destined to the lower-end of the domestic market at Hirose kiln at least until the late 1650s. The exploitation of Izumiyama's pure illitic clay started in the early 1650s and will enable Kakiemon I to fire the renowned milky-white nigoshide body at Kusunokidani and Kakiemon kilns. Arita potters appear to have established the practice of mixing heterogeneous grades of clays from different alteration zones as early as the 1620s, and continued to rely on such practice even after the discovery of the Izumiyama deposit, especially for mass-produced porcelains for both the domestic and European market.

Declaration of interests

The authors declare that they have no known competing financial interests or personal relationships that could have appeared to influence the work reported in this paper.

Funding

This research did not receive any specific grant from funding agencies in the public, commercial, or not-for-profit sectors.

Acknowledgements

We would particularly like to acknowledge Mr. Yoshihisa Tsuruta, Mr. Shuichi Tashiro and Mr. Kazuo Toyomasu for sharing their knowledge of raw materials, potting and firing techniques.

Appendix A. Supplementary data

Supplementary data to this article can be found online at https://doi.org/10.1016/j.oceram.2021.100217.

References

[1] O. Impey, The Early Porcelain Kilns of Japan, Clarendon Press, Oxford, 1996.
[2] T. Nagatake, Classic Japanese Porcelain - Imari and Kakiemon, Kodansha International, Tokyo, 2003.
[3] N. Murakami, Arita History and Folklore Museum - Excavated Ceramics, Exhibition Guidebook, 2021 (in Japanese).
[4] N. Murakami, The Origin of Imari Porcelain - Excavated Shards from Komizo Kiln, Sojusha Art Publishing, 2020 (in Japanese).
[5] R. Montanari, N. Murakami, M.F. Alberghina, C. Pelosi, S. Schiavone, The Origin of overglaze-blue enameling in Japan: new discoveries and a reassessment, J. Cult. Herit. 37 (2019) 94–102.

[6] R. Montanari, N. Murakami, P. Colomban, M.F. Alberghina, C. Pelosi, S. Schiavone, European ceramic technology in the Far East: enamels and pigments in Japanese art from the 16th to the 20th century and their reverse influence on China, Heritage Science 8 (1) (2020) 48.
[7] R. Montanari, M.F. Alberghina, A. Casanova Municchia, E. Massa, A. Pelagotti, C. Pelosi, S. Schiavone, A. Sodo, A polychrome Mukozuke (1624–1644) porcelain offers a new hypothesis on the introduction of European enameling technology in Japan, J. Cult. Herit. 32 (2018) 232–237.
[8] M. Nakagawa, Clay mineral associations and mineralogical properties of quartz in some pottery stones of western Kyushu, Japan, Appl. Clay Sci. 8 (1994) 331–347.
[9] Y. Kuwahara, S. Uehara, AFM study on surface microtopography, morphology and crystal growth of hydrothermal illite in Izumiyama pottery stone from Arita, Saga Prefecture, Japan, Open Mineral J. 2 (2008) 34–47.
[10] F. Bergaya, G. Lagaly, Handbook of Clay Science, second ed., vol. 5, Elsevier, 2013.
[11] M. Nakagawa, J. Nakamoto, T. Yoshihara, Hydrothermal alteration at the Izumiyama pottery stone deposit, Saga Prefecture - mineralogical properties of quartz and NH_4-bearing Sericite, Clay Sci. Soc. Japan 35 (1) (1995) 1–14 (in Japanese).
[12] N. Yoshida, J. Fukunaga, Mineralogical studies of Izumiyama pottery stone, J. Ceram. Assoc. Japan 70 (2) (1962) 36–41 (in Japanese).
[13] S. Higashi, Ammonium-bearing mica and mica/smectite of several pottery stone and pyrophillite deposits in Japan: their mineralogical properties and utilization, Appl. Clay Sci. 16 (2000) 171–184.
[14] G. Yanyi, Raw materials for making porcelain and the characteristics of porcelain wares in north and south China in ancient times, Archaeometry 29 (1) (1987) 3–19.
[15] Carolyn Kyongshin Koh Choo, Woong Kil Choo, Sangdoo Ahn, Young Eun Lee, Gyu Ho Kim, Yeon Sook Lee, A study of the chemical composition of Korean traditional ceramics (III): comparison of *punch'ŏng* with Koryŏ ware and chosŏn whiteware, J. Conserv. Sci. 27 (1) (2011) 75–90.
[16] F. Cavalcante, C. Belvisio, Argille e Minerali delle Argille – Trattamenti e metodi di preparazione di campioni di materiali argillosi per l'analisi diffrattometrica, in: Atti del VII Corso di Formazione dell'Associazione per lo Studio delle Argille (C.N. R.), Tito Scalo (PZ) 2004 V, 2005, pp. 23–50.
[17] D.M. Moore, R.C. Reynolds, X-ray Diffraction and the Identification and Analysis of Clay Minerals, Oxford University Press, New York, 1997.
[18] C.A. Jouenne, Traité de Céramiques et Matériaux Minéraux, Edition Septima, Paris, France, 1980.
[19] P. Colomban, J.P. Boilot, A. Kahn, G. Lucazeau, Structural investigation of protonic conductors NH4+ beta-alumina, New J. Chem. 2 (1978) 21–32.
[20] [Mercurio et al., 2019] M. Mercurio, F. Izzo, A. Langella, Metodi termici, in: Mariano Mercurio, Alessio Langella, Rosa Maria Di Maggio, Piergiulio Cappelletti (Eds.), Analisi Mineralogiche in ambito forense, Aracne Editrice, Roma, 2019, pp. 371–427.
[21] P. Colomban, Proton and protonic species : the hidden face of Solid State Chemistry. How to measure H-content in Materials, Fuel Cell. 13 (1) (2013) 6–18.
[22] K.K. Turekian, L. Kulp, The Geochemistry of Strontium, Geochimica and Cosmochimica Acta, vol. 10, Pergamon Press Ltd, London, 1956, pp. 245–296.
[23] G. Faure, J.L. Powell, Strontium Isotope Geology, Springer, Verlag Berlin - Heidelberg - New York, 1972.
[24] R. Kerr, N. Wood, Science and Civilisation in China: Volume 5, Chemistry and Chemical Technology, Part 12, Ceramic Technology, Cambridge University Press, Cambridge, 2004.
[25] H. Ma, J. Henderson, J. Evans, A new method of identifying the flux in ancient Chinese high fired glaze - Sr Isotopic composition analysis, World Scientific, Ser. Archaeol. Hist. Sci. China Volume 2 (2016) 353–373 (Chapter 18).
[26] T. Kondo, On the chemical constituents of the heart wood of distylium racemosum s. et z, J. Fac. Agric. Kyushu Univ. 10 (No. 1) (1951).
[27] M. Fitski, Kakiemon Porcelain - Handbook, Leiden University Press, Leiden, 2011.
[28] D. Mohapatra, D. Mishra, G.R. Chaudhury, R. Prasad Das, Arsenic adsorption mechanism on clay minerals and its dependence on temperature, Kor. J. Chem. Eng. 24 (3) (2007) 426–430.
[29] A. Violante, M. Pigna, Competitive Sorption of arsenate and Phosphate on different clay minerals and Soils, Soil Sci. Soc. Am. J. 66 (6) (2002) 1788–1796.
[30] S. Goldberg, Competitive adsorption of arsenate and arsenite on oxides and clay minerals, Soil Sci. Soc. Am. J. 66 (6) (2002) 413–421.
[31] B.A. Manning, S. Goldberg, Modeling arsenate competitive adsorption on kaolinite, montmorillonite and illite, Clay Clay Miner. 44 (5) (1996) 609–623.
[32] Kysuhu Ceramic Museum, in: Kakiemon - the Whole Aspect of the Kakiemon Style - Special Exhibition, 1999 (in Japanese).